

# Pre-operative Planning and Intra-operative Guidance for Shoulder Replacement Surgery

Charl P. Botha<sup>1,3</sup>, Peter R. Krekel<sup>1,2</sup>, Edward R. Valstar<sup>2</sup>,  
Paul W. de Bruin<sup>3</sup>, P. M. Rozing<sup>2</sup>, and Frits H. Post<sup>1</sup>

- 1 Department of Mediamatics, Delft University of Technology, The Netherlands  
[{c.p.botha,f.h.post}@tudelft.nl](mailto:{c.p.botha,f.h.post}@tudelft.nl)
- 2 Department of Orthopaedics, Leiden University Medical Centre, The Netherlands  
[{p.r.krekel,e.r.valstar}@lumc.nl](mailto:{p.r.krekel,e.r.valstar}@lumc.nl)
- 3 Department of Radiology, Leiden University Medical Center, The Netherlands  
[{p.w.de\\_bruin,p.m.rozing}@lumc.nl](mailto:{p.w.de_bruin,p.m.rozing}@lumc.nl)

---

## Abstract

---

Shoulder joint replacement, or arthroplasty, is indicated in cases where arthritis or trauma has resulted in severe joint damage that in turn causes increased pain and decreased function. However, shoulder arthroplasty is less successful than hip and knee replacement, mostly due to the complexity of the shoulder joint and the resultant complexity of the replacement operation.

In this paper we present a complete visualization-oriented pre-operative planning and intra-operative guidance approach for shoulder joint replacement. Our system assists the surgeon by allowing a virtual arthroplasty procedure whilst giving feedback, primarily via patient- and procedure-specific joint range of motion (ROM) simulation and visualization. After a successful planning, our system automatically generates a 3D model of a patient-specific mechanical guidance device that is then produced by a rapid prototyping machine and can be used during the operation. In this way, a computer-based guidance system is not required in the operating room.

**1998 ACM Subject Classification** I.3.8 Applications, J.3 Life and Medical Sciences

**Keywords and phrases** Surgery Assistance

**Digital Object Identifier** 10.4230/DFU.SciViz.2010.179

## 1 Introduction

Rheumatoid arthritis and osteoarthritis, the two most common forms of arthritis, are diseases that adversely affect joint cartilage and bone quality. They can lead to severe joint damage that in turn causes increased pain and reduced joint mobility and patient function. In these cases, joint replacement is indicated. Joint replacement, or arthroplasty, is a surgical procedure during which diseased parts of a joint are removed and replaced with artificial components.

Hip and knee replacements are successful procedures with regard to pain relief, post-operative joint functionality and durability. At ten years follow-up, the revision rate for cemented total hip prostheses is 7% and about 13% for uncemented total hip prostheses [15]. In contrast to this, shoulder replacement yields good results with regard to pain relief, but fares significantly worse with regard to post-operative joint functionality and especially replacement durability. Literature shows that after nine years, between 24% and 44% of shoulder glenoid components show radiological loosening [22], i.e. loosening that is visible on a radiograph.

 © C. P. Botha, P. R. Krekel, E.R. Valstar, P. W. de Bruin, P. M. Rozing, F. H. Post;  
licensed under Creative Commons License NC-ND

Scientific Visualization: Advanced Concepts.  
Editor: Hans Hagen; pp. 179–195

 Dagstuhl Publishing  
FOLLOW-UPS Schloss Dagstuhl – Leibniz Center for Informatics (Germany)

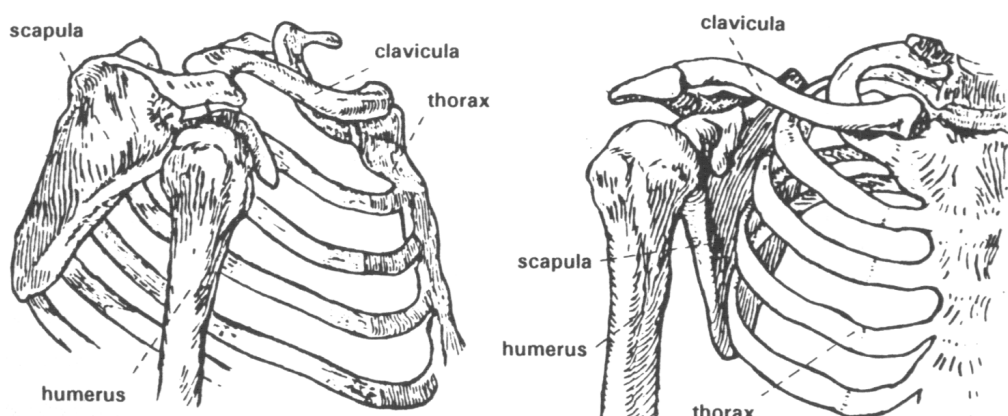


**Figure 1** The skeletal structures of the shoulder. Illustration courtesy of the Delft Shoulder Group.

One of the reasons for this situation is the fact that the placement of shoulder prostheses is a difficult procedure. The procedure is complicated by two factors:

- The shoulder joint is a more complex mechanism than either the hip or the knee joints.
- A relatively small incision is made during the shoulder replacement operation. This small incision results in a limited field of view for the surgeon.

Figure 1 shows the skeletal structures in the human shoulder. The upper arm bone, or humerus, rotates against the glenoid, which is the shallow cup-like part of the shoulder-blade, or scapula. The humerus is held in the shoulder joint by a collection of muscles and tendons called the rotator cuff. The scapula itself is non-rigidly attached to the thorax via the collar-bone, or clavicula, and is able to slide over the thorax.

This flexible construction yields an impressive range of motion (ROM) for the shoulder joint, but as is almost always the case with increased complexity, is less robust than for instance the hip joint. The complexity of the shoulder joint contributes to the difficulty of performing a good replacement. Besides the fact that the precise functioning of this joint is not entirely clear, the surgeon has to cope with extremely limited visibility during the replacement operation. These factors contribute to the lower long-term success-rate of shoulder replacement.

In shoulder replacement, or shoulder arthroplasty, the humeral head and the glenoid are replaced with prostheses. Figure 2 shows an illustration of the skeletal structures in the human shoulder with implanted glenoid and humeral head prostheses.

Currently, the de facto standard for pre-operative planning for shoulder replacement is template-over-x-ray planning. The orthopaedic surgeon manually overlays transparencies with various prosthesis sizes and types on an x-ray of the patient's shoulder. Consequently, the surgeon decides on a particular prosthesis type and size, based only on a two-dimensional projection of the bony anatomy of the shoulder. In addition, this method of planning offers no patient-specific intra-operative guidance for prosthesis placement.

In order to improve the existing planning approach and hence also the outcome of shoulder replacement surgery, we have developed a flexible prototype surgical planning software system as well as linked mechanical guidance devices, also called patient-specific templates. The replacement operation is planned by making use of our pre-operative planning software. Integrating patient-specific joint motion simulation, the software is able to predict the post-

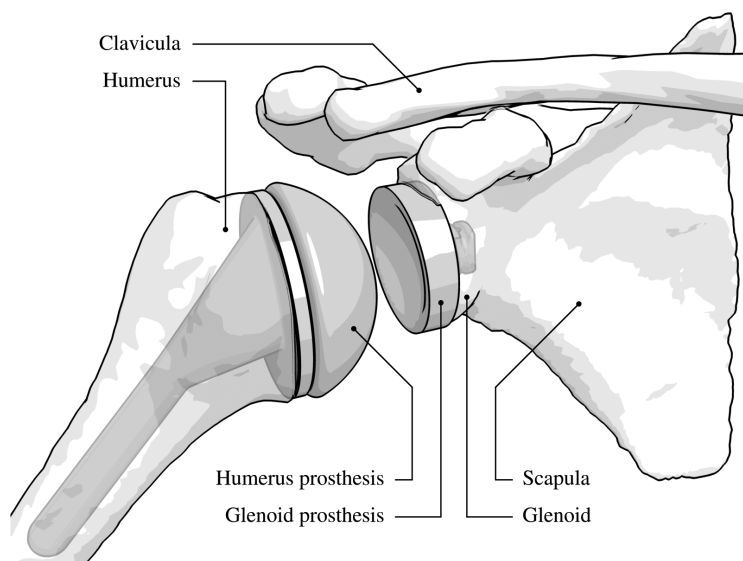


**Figure 2** Illustration of a shoulder after an arthroplasty. Both the humeral head and glenoid prostheses have been virtually implanted, i.e. a total shoulder replacement has been performed.

operative patient joint range of motion (ROM). Based on this, the surgeon can optimize their planning. The parameters of the virtually performed operation, such as the insertion position and angle of the glenoid component, are used to design a patient-specific mechanical guidance device that is manufactured with rapid-prototyping techniques. The guidance device uniquely docks with easily identifiable bony structures in the patient's shoulder and is used for robust mechanical intra-operative guidance.

In this paper, we collect a number of our recent advances and show how they are integrated to form a complete pipeline for the pre-operative planning and intra-operative guidance of shoulder arthroplasty surgery. We present a new approach for the segmentation and accurate surface extraction of the bony structures from CT data of shoulder replacement patients. Due to its pathology, segmentation of the data offers unique challenges. However, the segmentation is required for the subsequent simulation steps. We then document the pre-operative approach we have developed, including the real-time post-operative joint range of motion (ROM) prediction and visualization. Finally, we show how the planning information can be used to design a patient-specific mechanical guidance device for glenoid component replacement. The range of motion simulation has been published elsewhere [13], and the idea of the shoulder guidance device has been presented previously [23]. The contribution of the present article consists of the shoulder segmentation technique, the *automatically* designed guidance devices and the integrated shoulder replacement planning and guidance pipeline.

## 2 Previous Work

We discuss previous and related work in two parts. In the first part we give an overview of techniques related to joint segmentation and in the second part we focus on planning and guidance for joint replacement.

## 2.1 Joint Segmentation

In previous research we developed a technique to determine the radius and centre of the humeral head using a modified Hough transform [24]. This is an effective approach and might be combined with our current work, but for pre-operative planning and ROM simulation we require complete and accurate surface representations of the skeletal structures in the shoulder.

Branzan-Albu et al. presented an approach to segment the skeletal structures from T1-weighted MRI images of healthy shoulders [3]. A separate segmentation was performed on each 2D slice and the results are combined to form a smooth 3D segmentation. The results are good but this technique has been developed for healthy shoulders with large joint space width and healthy bone density. In addition, it focuses on a small region of interest around the gleno-humeral joint.

A general approach for segmenting skeletal structures from CT data was presented by Kang et al. [11]. This approach is based on 3D region growing with locally adaptive thresholds following by a mixture of 3D and 2D morphological operations to close holes in the segmented surfaces. The resulting segmentation is then smoothed by adjusting its containing iso-surface. The approach is applied on the hip, the knee and the skull. The authors state that a site-specific approach is required for separating different bony structures at joints before their techniques can be applied. In the case of the hip, they make use of a manually-placed sphere. In our opinion, the determination of this site-specific separation method is one of the most complex tasks in the case of the shoulder.

Zoorofi et al. segmented hip joints by making use of histogram-based thresholding and an interesting hip-specific approach based on the convex hull of the initial thresholding and the application of the Hough transform [26]. This is a promising technique, but is very much hip-specific.

There are a number of examples in literature on segmenting skeletal structures from CT data, but very few of these address the problem of separating neighbouring skeletal structures, such as those found in joints. If we further narrow the problem to that of separating neighbouring skeletal structures from pathological CT data, even fewer examples remain. When we add the extra specification that it should deal with shoulder joints, there's almost nothing to be found. Our work attempts to fill this important and unexplored research area.

## 2.2 Planning and guidance for joint replacement

A wide range of pre-operative planning systems exist, for example Hip-Op [14], HipNav [20] and BrainLAB's VectorVision<sup>1</sup>. However, to our knowledge no such specific planning system for the shoulder joint is available at this time. Probable factors here are the complexity and the relatively lower number of replacements of the shoulder joint.

Most surgical guidance systems with a computer-based pre-operative planning stage make use of optical tracking systems during surgery. In our case, we couple computer-based pre-operative planning with automatically designed patient-specific mechanical guidance devices. The idea of manually designing patient-specific guidance devices or templates for surgical guidance has been explored for spinal surgery [7]. Our first manual designs for the shoulder guidance device have been presented [23]. In this article we present the first example

---

<sup>1</sup> <http://www.brainlab.com/>

of an automatically designed patient-specific guidance device that can be produced using rapid-prototyping techniques.

### 2.2.1 Range of Motion simulation

Joint range of motion (ROM) simulation aims to predict the post-operative motion patterns of a patient joint, based on pre-operative medical image data and the parameters of the planned surgical procedure.

Some research has been done on pre-operative ROM estimation for the hip joint. Jaramaz et al. use analytical modeling of the properties of implants to estimate both the ROM and the chance of dislocation, with bony impingement hardly playing a part [10]. The approach of Richolt et al. resembles our approach more closely, by applying collision detection to the 3D problem of bony impingement [17]. Their system is designed for osteotomy rather than joint replacement and only determines ROM for joint rotation along a single user-defined axis.

The simulator we describe in this paper predicts bone-determined ROM, i.e. soft tissue is not taken into account. For a full arthroplasty simulator we would require additional information on the presence of muscle tissue, ligaments and cartilage. Alternatively, a model of these aspects could be used, such as the Delft Shoulder and Elbow Model (DSEM) [25]. This is a musculoskeletal model of the shoulder and elbow joint that mainly focuses on muscle function and the involved forces and energy. However, the DSEM is not patient-specific.

In section 4.2 of this article we present a summary of our previous ROM prediction and visualization work [13] in order to serve as context for the full planning and guidance system.

## 3 Segmentation

The pre-operative planning, and especially the ROM simulation component, require high-quality surface meshes describing the bony surfaces in the human shoulder. These surfaces have to be extracted from CT data of patients with bone- and cartilage-affecting diseases. This, together with the complex geometry of the shoulder joint, results in a complex segmentation problem. Figure 3 shows a single axial slice from a typical dataset. In this case, joint space narrowing caused by arthritis results in the humerus and the scapula appearing fused. Decalcification, also related to the disease, in addition to the partial volume effect, leads to edges that are fuzzy and difficult to detect. Traditional approaches fail completely on this data.

Our approach combines a number of powerful techniques to separate complex touching structures by masking and inverse masking, then extracting initial surfaces that are larger than the objects that we wish to segment, and subsequently deflating deformable surfaces to fit precisely on the outside surface of those objects, all the while preserving the topology of the deforming surfaces [2]. Figure 4 is a flow chart illustrating the complete approach. In the following subsections, we will briefly explain each of these stages.

### 3.1 Deriving structure masks

The first step is to derive conservative structure masks for the structures that are to be segmented and in some cases also for structures that border on those that are to be segmented. We define a conservative structure mask as a list of *all* contiguous voxels that can be reasonably assumed to be contained within the boundaries of the structure that is being masked. Our use of *conservative* indicates that we prefer false negatives over false positives. In other

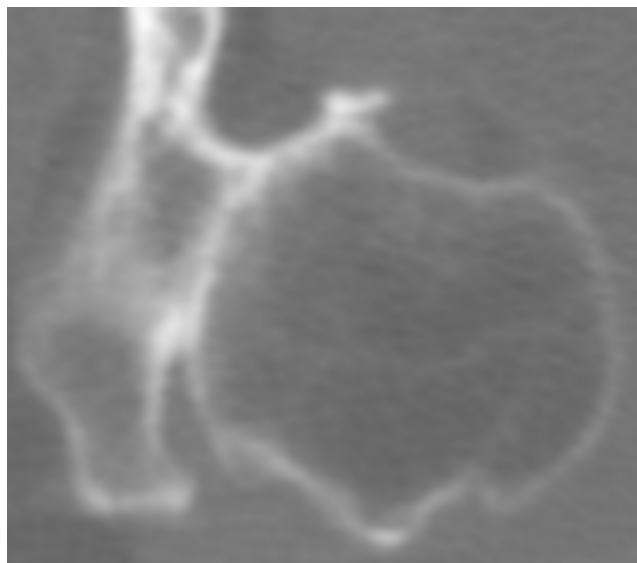


**Figure 3** An axial slice from an arthritic shoulder CT dataset showing a humeral head and a scapula that appear to be fused together. This is due to the joint space being extremely narrow and the limited resolution of the CT scanner.

words, we prefer a mask that does not fully cover the structure of interest over one that covers the structure as well as some of its surroundings.

We use two main methods to generate these masks, indicated by the grey blocks marked *A* and *B* in Figure 4. Method *A* is used if structures do not touch and method *B* is used if they do. In most cases, both methods are used to generate a library of masks for each dataset. These masks can be combined to activate or to deactivate arbitrary parts of the dataset.

### 3.1.1 Method A

This method starts with an interactive histogram segmentation. This method is similar to that described in [9] and based on concepts presented in [12] and [18]. It makes use of a linked, or coupled, view that shows a 2-D histogram of image gradient magnitude over image intensity for the CT data that is being examined. By delineating regions on this histogram with closed polygons or splines, the user can select data points on the basis of both their intensity and gradient magnitude.

After this step, other masks from the library (for example generated by method *B*) can be used to remove unwanted components of the selection. Followed by a connected components analysis and our modified hole filling algorithm, filled and contiguous structure masks can be generated. Our modified hole filling algorithm is a standard morphological binary reconstruction hole-filling algorithm where we modify the conventional marker image to deactivate one or more of the volume boundaries. By doing this, we allow for expected open cavities, such as the interior of the humerus, to be filled as well.

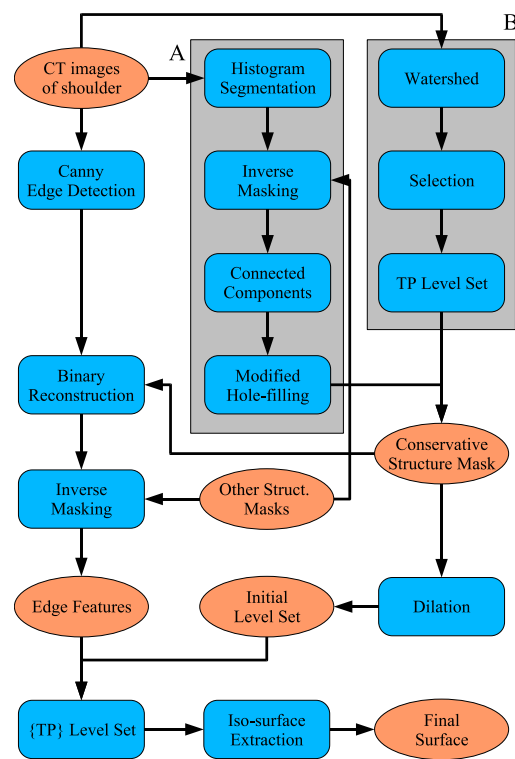


**Figure 4** A flow chart illustrating our approach to the segmentation of the skeletal structures of the shoulder. Ovals signify data and blocks signify operations. The *A* and *B* blocks show two distinct ways to generate the initial conservative bone mask. *TP* signifies *Topology Preserving*. All these operations take place in 3D.

### 3.1.2 Method *B*

Starting with a 3D morphological watershed and basin merging step, this method is able to do an initial separation of touching complex objects, such as the humerus and scapula shown in Figure 3. During an interactive selection step, the user indicates which of the merged watersheds are relevant. The selected watersheds are combined and are used as an initial implicit surface during a level-set [19] based surface inflation step to refine the structure mask. The surface is inflated until it reaches the inside edge of bony structure that surrounds it.

## 3.2 Deformable surfaces

A 3D Canny edge detection [4] is applied to the input data. With the correct thresholds, this yields a volume containing a number of edge voxels. For each bony structure that we segment, we perform a morphological binary reconstruction of the edge voxels from the conservative mask for that structure. This operation removes all edge voxels that are disconnected from those voxels that touch the mask directly or indirectly (via connections with other edge voxels). Again masks from the library can be used after this step to remove any remaining edge voxels that are not relevant to the structure that we are segmenting. The result is a volume with voxels that are zero everywhere, except on the edges of the structure of interest where the voxels have unit value.

The conservative structure mask of the bony structure that we are segmenting is dilated so that it completely envelops all edge features. The dilated mask is converted to an implicit surface and then deflated using a topologically constrained [8] geodesic active contour [5] using the inverse of the edge features described above as the speed function. In other words, the speed function has unit value everywhere, except on the edges, where it has value zero. This causes the level set to continue deflating until it reaches an edge. The outside surface of both the scapula and the humerus have a topological genus of 0 in the majority of cases. We have integrated this knowledge into the segmentation pipeline by ensuring that we start with a genus 0 initial surface and constraining its topology as it deforms. This technique solves a number of problems related to the thinness and complexity of the scapula and the relatively low resolution of the CT data by preventing holes or isolated points from forming.

The segmentation process is repeated for each of the bones that need to be extracted. In general, we require models of the scapula and the humerus for pre-operative planning and ROM simulation.

## 4 Pre-operative Planning

During the planning phase, the glenoid and humeral components have to be selected and virtually implanted. During the virtual implantation, the system presents feedback to the surgeon about the structural quality of the planned procedure, e.g. whether there is sufficient contact between the prosthesis and the bone, as well as the functional quality of the planned procedure. Our system also simulates and visualises the ROM of the patient shoulder.

### 4.1 Virtual implantation

Docking two 3D objects using only a perspective or an orthogonal projection on a conventional screen is by nature quite difficult. In our case, we need precise control over the position and orientation of a prosthesis in order to implant it virtually into the surface model of the scapula.

In order to solve this problem, we made use of some basic CAD interaction techniques combined with the practical techniques used by orthopaedic surgeons during shoulder replacement surgery. Refer to Figure 5 during the following explanation. During a conventionally planned shoulder operation, the orthopaedic surgeon initially tries to align the glenoid prosthesis with the intersection between two imaginary planes. The first plane passes through the centre of the glenoid and the most lateral edge of the scapula. The second plane is roughly orthogonal to the first, parallel to the spine and passes through the centre of the glenoid. Experience has shown that this will help to achieve a post-operative centre of gleno-humeral rotation that is close to, or coincides with, a healthy centre of rotation. This result plays a very important role in the success of the replacement [6].

The planning software integrates a range of geometrical constraint-based object manipulation techniques based on points, axes and planes. With this functionality, the double plane insertion sketched above can easily be constructed and used as a first estimate for glenoid component placement. In order to do this, the surgeon will start by selecting three points: one in the centre of the glenoid and two on the lateral edge of the scapula. These points are shown in Figure 5a and are marked with respectively “Glenoid”, “Lateral 1” and “Lateral 2”. The point selection logic makes it easy to select points on surfaces and will also keep these latched to the surface when they are moved. A scapula lateral edge slice can now be created by making use of these three points as a plane definition. The system will warn if the three selected points do not uniquely define a plane. See Figures 5 and 6 for an example

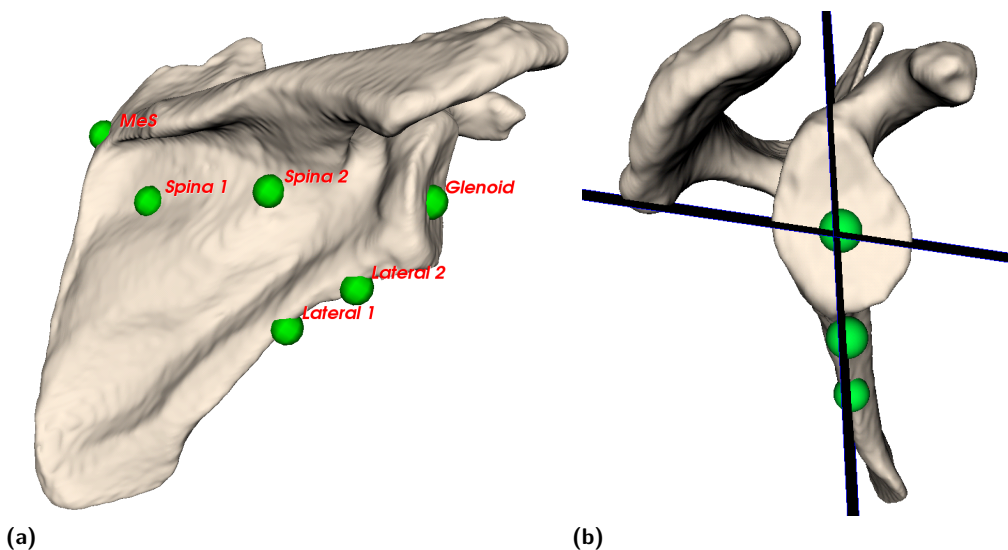


**Figure 5** In (a), a scapula is shown with the points that are required to place the two anatomical planes. In (b), the same scapula is shown with the resultant anatomical planes intersecting to form an insertion axis for the glenoid prosthesis.

of such a plane intersecting the scapula. It can also happen that the plane defined by these three points does not have the desired orientation. In our experience, substituting one of the lateral edge points with the point where the spina meets the medial edge of the scapula, labeled “MeS” in Figure 5a, solves this problem.

By repeating this process, but instead making use of the point on the centre of the glenoid and two points on the posterior side of the scapula approximately equidistant from the spina, a second plane can be defined. These two extra points are labeled “Spina 1” and “Spina 2” in Figure 5a. The intersection of these two planes constitute a very good first estimation of the glenoid insertion axis. This plane intersection is shown in Figure 5b.

The constraint system can now automatically align the prosthesis axis with the intersection of the two planes and optionally constrain all prosthesis motion to the plane intersection. The object with the horizontal pin in Figure 6a represents the glenoid prosthesis. Logically the constraint system can also work with a single plane: in this case the prosthesis can be aligned with the plane, i.e. be embedded in it, and optionally all prosthesis motion can be constrained to the plane. This is the approach that has been chosen in Figure 6.

During the final prosthesis manipulation, objects can be hidden and object contouring activated, so that the object intersection curves with the anatomical planes can be seen overlaid on the CT-data slices. This is shown in Figure 6b. In this mode, the volume slice can still be moved to and fro. This enables the surgeon to judge the fit of the prosthesis with regard to the bone volume that is visible in the CT-scan. This view is more familiar to surgeons, as it is strongly reminiscent of the template-over-x-ray planning method.

The humeral prosthesis is placed in accordance with the actual surgery. During the procedure, a metal ring is fitted on the humeral head. This defines the location of the centre of rotation as well as the size of the humeral prosthesis. A pin is drilled into the bone through a guidewire at the center of the ring. On this pin a metal block is mounted. When sawing off part of the humeral head, the surgeon follows the plane as imposed by the metal block.

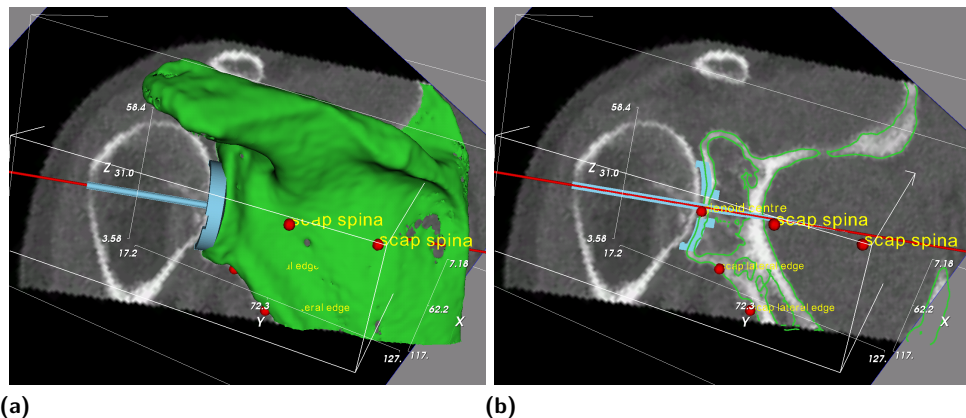


**Figure 6** Part of the glenoid component planning functionality. In (a) the complete models are shown and in (b) only their contours. The contour view enables the user to judge whether the prosthesis has a good fit and is reminiscent of the conventional template-on-x-ray planning. The slice is anatomically oriented but can be moved to check all parts of the glenoid component.

In the pre-operative planning system, we fit a sphere through the humeral head. Virtual models of the pin and metal block are positioned using the centre of rotation defined by the sphere. The cutting plane defined by the metal block is applied and the prosthesis is placed at the centre of the intersection plane. This completes the placement of the prosthesis. All of the parameters can be adjusted at any time during the simulation.

## 4.2 ROM simulation and visualization

Throughout the surgeon's interaction, the predicted patient-specific range of motion (ROM) can be calculated and visualized [13]. The ROM is bone-determined in that only the bone geometry plays a role in the simulation. Soft tissue does not play any role. The gleno-humeral ROM is visualized with motion envelopes, that indicate the maximum ROM of the humerus in every direction. In addition, a novel visualization technique depicts the differences between the current and previous ROM during the surgeon's interaction.

In order to calculate the ROM using a segmented CT dataset, we implemented a simplified bio-mechanical model of the gleno-humeral joint. A generally accepted hypothesis is that the gleno-humeral joint can be approximated by a ball-joint [16, 24]. We combined this model with collision-detection on surface models of the skeletal structures in the patient's shoulder.

Our simulator is capable of handling hemi-prostheses, which is a prosthesis without a glenoid component, and also reversed prostheses, where the spherical component is placed at the glenoid.

For all prostheses, the ROM envelopes are constructed in the following way. The humerus is aligned with an initial orientation, which will be the starting alignment for all iterations. The simulation consists of two nested iterations. During the outer iteration, the humerus is rotated around the axis marked with  $A_i$  in Figure 7. Axis  $A_j$  rotates along with  $A_i$ .

At each rotation, the maximum possible orientation of the humerus around axis  $A_j$  is found by making use of a binary search. By repeatedly dividing the search interval in half, our ROM determination executes in  $O(\log n)$ , where  $n$  relates to the effective resolution of the end result of the binary search. Whenever colliding polygons are detected, we reverse the

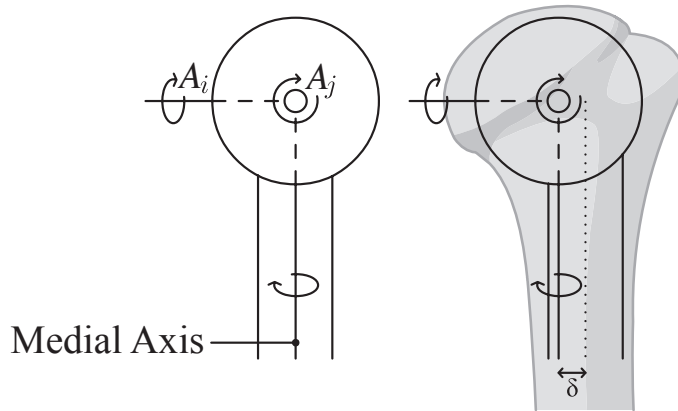


**Figure 7** A schematic representation of the humerus and its rotational axes. As can be seen in this image, the additional ROM as the result of endo/exorotation is related to  $\delta$ , the distance between the medial axis of the humerus and the vertical axis through the center of rotation.

search direction. We use OPCODE [21] (Optimized Collision Detection), an efficient library based on memory-optimized bounding-volume hierarchies to detect colliding polygons.

A complete new ROM has to be determined for each change made by the surgeon that affects the bone or prosthesis geometry, for example a change in the position of the humeral prosthesis.

In order to enable the real-time use of the ROM simulation, we have developed two optimization approaches. In the interpolation approach, a large number of ROM envelopes are precalculated so that ROM envelopes can be interpolated during interaction. In the collision clipping approach we make use of a clipping plane to clip collisions, thus rendering the usual re-initialization of the collision detection data structures during each ROM calculation unnecessary. This same clipping plane is uploaded to the graphics hardware to clip the geometry.

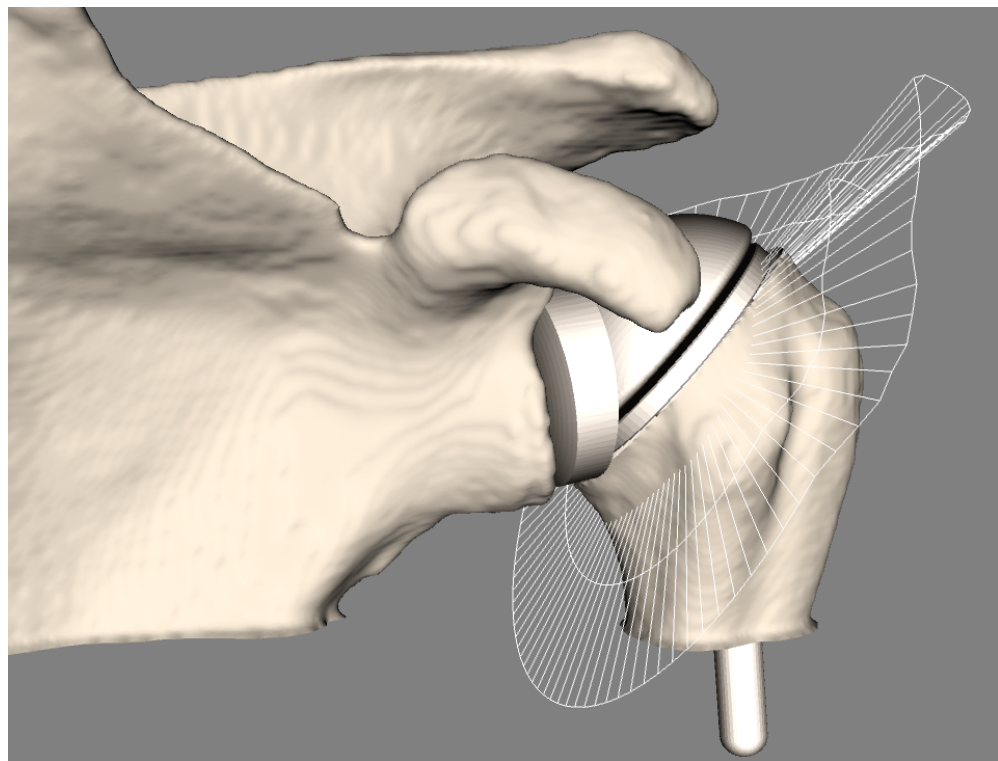
#### 4.2.1 Visualization

Once all directions of our ROM envelope have been probed for their maximum angles, we can begin constructing the ROM visualization. We draw lines between the center of rotation and an arbitrary point within the end of the shaft of the humerus, and then transform these lines according to their respective maximum angles. The resulting envelope is shown in Figure 8.

For each change made to the virtual prosthesis placement by the surgeon, a new ROM envelope is calculated and visualized. This enables the surgeon to visualise directly the complete shoulder ROM for a particular set of operational parameters. Being able to see the envelope update in real-time as changes are being made, helps the surgeon to investigate the effect of even small changes to the planned operation.

Several parameters that define the placement of the humerus prosthesis can be adjusted during the interaction. First of all, the cutting plane at the humeral head can be translated along its normal, as well as rotated around two axes perpendicular to the normal. Also, the position of the humerus prosthesis relative to the humerus can have a small offset in any direction within the cutting plane.

In general, the placement of the glenoid component is constrained by the quality and the



■ **Figure 8** The visualization of ROM by means of envelopes.

geometry of the scapula and takes place according to the method described in Section 4.1. Therefore our ROM simulation and visualization focuses on changes in the humeral component placement, but applying it to glenoid placement changes would be straight-forward.

In order to facilitate this important investigation of the increase or decrease in ROM that results from a particular change in the planning, we have implemented comparative visualization functionality whereby the difference between two ROM envelopes can be explicitly visualized. The comparative visualization is also updated in real-time as the surgeon interacts with the planning.

For two consecutive envelopes we depict improvements and deteriorations by connecting the lines with colored polygons. A red polygon denotes that the most recent envelope has a more limited ROM in that particular direction than the reference envelope, while a green polygon states the opposite. Additionally, the end points of the lines are connected with arrows, pointing towards the most recent envelope. The resulting visualization is shown in Figure 9. The reference envelope can be set to the current or any previously determined ROM envelope at all times.

## 5 Guidance Device

The guidance device is a crucial link between the pre-operative planning phase and the execution of the procedure in the operating room. During pre-operative planning, the size and type of prosthesis can be determined and this knowledge can easily be applied during the actual replacement. Prosthesis position and orientation, however, require some extra ingenuity.

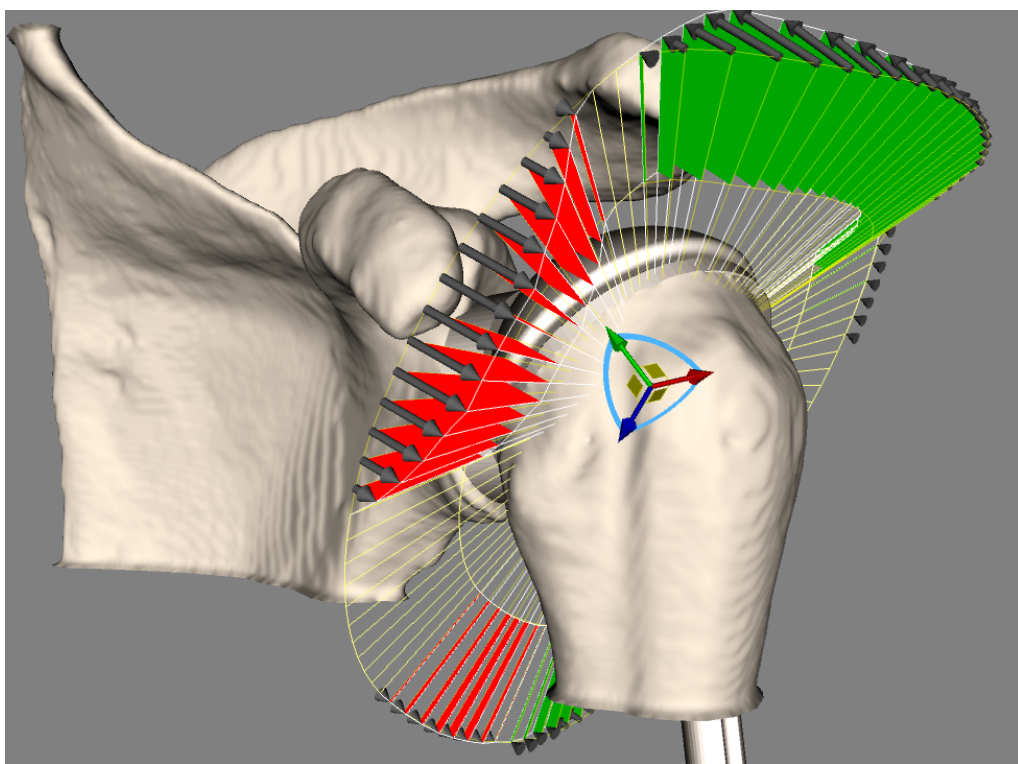


**Figure 9** Comparative visualization of two ROM envelopes. The first envelope is a previously determined ROM which was set as a reference envelope by the user. The second envelope is continuously updated for every adjustment applied to the prosthesis placement parameters.

In order to realise this planning in the operating room in a robust and efficient fashion, we are working on applying principles for the design of pedicle screw drill guides [7] to the design of a patient-specific guidance device for shoulder replacement.

The patient-specific mechanical guidance device is a jig, or template, that can be used by the surgeon during the operation to guide the use of another tool such as a drill or a pneumatic saw. In the case of a glenoid replacement, the template uniquely fits the patient's scapular glenoid and has a conduit for a drill, thus acting as a drill-guide. By making use of this template, the surgeon can ensure that the pre-operatively planned glenoid insertion position and orientation are realized. In this way, a cheap and robust coupling between the computer-based intra-operative planning and the operation itself is realized.

Figure 10a shows the latest design of our glenoid drill guide. Figure 10b shows a guidance device that our planning software has designed for the patient and the planned implantation. The guidance device is manufactured with a rapid-prototyping machine.

## 6 Results

In order to evaluate the results of our segmentation approach, we started by comparing its results on an experimental CT dataset of an *ex vivo* scapula to a manual expert segmentation. The manual segmentation was performed by drawing a contour describing the outside scapular surface on each axial slice of the  $512 \times 512 \times 420$  dataset, sampled at a resolution of  $0.333 \times 0.333 \times 0.5\text{mm}$ , and then linking these contours together with triangles. The resultant mesh consisted of 6900 triangles, was closed and it was of genus 0 topology.

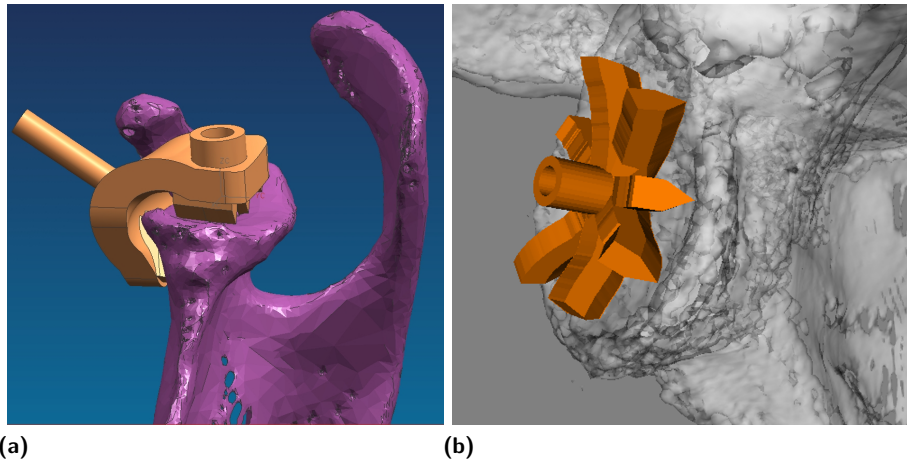


**Figure 10** In (a), the latest design of the glenoid drill guide is visualized on a surface model of a scapula, courtesy of Liesbet Goossens and Bart de Schouwer, Katholieke Universiteit Leuven, Belgium. In (b), another design that has been automatically made patient-specific by the planning software is shown.

We used our method to segment the scapular mesh from the same data. The resultant mesh consisted of 729212 triangles, was closed and was also of genus 0 topology. The large number of triangles is the usual result of applying the Marching Cubes algorithm to a volume of this resolution to extract a surface of this complexity. We did not apply any decimation techniques to the mesh.

We compared the meshes using the Mesh software [1]. The maximum, mean and root-mean-squared (RMS) symmetric Hausdorff distances are 3.7, 0.4 and 0.5mm respectively. The symmetric distance is the maximum of the distances from the first mesh to the second mesh and from the second mesh to the first. The distances as a percentage of the largest diagonal of the bounding box of the scapula are 1.6, 0.2 and 0.2% respectively. The RMS error is in the order of a single voxel. We find this result quite acceptable for a manual vs. automatic reconstruction.

Most of the outliers, and specifically the parts of the mesh that cause the maximum Hausdorff distance, are caused by cartilage being misclassified as cortical bone. This is especially a problem with cadaveric material, as the cartilage seems to harden over time and thus appears in the CT data with greater intensity.

We have also tested the complete prototype planning system, including the segmentation, on a number of in-vivo shoulder CT datasets of patients requiring total shoulder replacements. Feedback from the operating orthopaedic surgeon, who used the system primarily for pre-operative exploration, was positive. The fact that our bone-determined ROM simulation can be used to predict impingement, i.e. when due to prosthesis placement joint motion is restricted by bone colliding with bone, is seen as particularly important.

We benchmarked the interactive performance of the ROM simulator on a Pentium 4 running at 2.66 GHz with 512 MB of RAM. The humerus model consisted of 50.000 polygons, while the scapula consisted of 155.000 polygons.

Performance figures for the interactive ROM simulation are listed in Table 1. As can be seen, the speed increase due to collision clipping varies from a factor of 1.33 to 8.22 for normal usage of the simulator. The speed increase due to interpolation varies from a factor of

**Table 1** Speed of simulation and rendering in updates per second. All performance figures are specified as updates per second, figures in parentheses refer to speedups relative to “no optimization” performance.

	With rendering	Without rendering
no optimization	0.27	0.30
collision clipping	2.22 ( $\times 8.22$ )	2.69 ( $\times 8.97$ )
interpolation	10.81 ( $\times 40.04$ )	374.4 ( $\times 1248$ )

10.74 to 40.04. If we discard the graphical representation, the speed increase by interpolation gets as high as a factor of 1248.

The precalculation interpolation optimization leads to a great speed-up, but can only be used if sufficient time for pre-processing is available (approximately 20 minutes for the cases presented here) and if the surgeon’s changes are limited to a known set of possibilities. The collision clipping optimization leads to a less significant speed-up, but can be applied in all cases and does enable the interactive use of the ROM simulation.

We have performed initial validation experiments on cadaver scapulae to test the design and functioning of the drill-guide [23]. The results were promising, but do require improvement, as the cartilage covering the glenoid has a significant impact on the orientation of the resultant implant. The drill guide is designed based on the bony surface of the glenoid and not the cartilage covering it. Cartilage will be taken into account in future experiments.

## 7 Conclusions and Future Work

In this paper we have described a complete visualization-oriented process for the pre-operative planning and intra-operative guidance of shoulder replacement surgery.

We presented an approach for segmenting the bony structures from CT data of arthritic patients. Existing methods, mostly designed for other joints, all fail on this type of data. We then showed how these segmentations are used in an interactive pre-operative planning solution that assists the surgeon in virtually implanting shoulder prostheses. The pre-operative planning software gives real-time feedback on structural and functional aspects of the planned procedure. The bone-determined shoulder ROM is calculated and visualized interactively, so that the surgeon gets feedback on every small change made to the planning. Changes in ROM are also explicitly visualized, helping the surgeon to fine-tune the planning.

The CT data and pre-operative planning are used to automatically generate a patient-specific mechanical guidance device that can be used during the replacement operation to execute the planning. To increase accuracy and reliability of the guidance devices during surgery, we will focus on improved imaging of cartilage, and refine the modelling to improve mechanical support from the cartilage.

We are currently working on a new segmentation approach that exploits image-based curvature in combination with a priori knowledge of the shoulder anatomy, leading to more robust and accurate segmentation results.

The ROM simulator will be further refined to include effects of soft tissue and active motion on joint mobility. Reference standards for mobility of healthy joints will be developed to estimate the amount of functionality to be restored after joint replacement. We are currently validating aspects of the ROM simulator as part of a cadaveric study.

We are also preparing for a series of clinical studies in using our pre-operative planning system for actual replacement surgery. A thorough evaluation of all stages of the pipeline

will be carried out, including post-operative functional tests, to compare the overall results of the process with current clinical practice.

---

**References**

---

- 1 N. Aspert, D. Santa-Cruz, and T. Ebrahimi. Mesh: Measuring error between surfaces using the Hausdorff distance. In *Proceedings of the IEEE International Conference on Multimedia and Expo 2002 (ICME)*, pages 705–708, 2002.
- 2 Charl P. Botha. *Techniques and Software Architectures for Medical Visualisation and Image Processing*. PhD thesis, Delft University of Technology, 2005.
- 3 Alexandra Branzan-Albu, Denis Laurendeau, Luc Hébert, Helene Moffet, Marie Dufour, and Christian Moisan. Image-guided analysis of shoulder pathologies: Modeling the 3D deformation of the subacromial space during arm flexion and abduction. In Dimitris Metaxas Stephane Cotin, editor, *International Symposium on Medical Simulation (ISMS 2004)*, volume 1 of *Lecture Notes in Computer Science*, pages 193–202, Cambridge, MA, USA, June 17-18 2004. Springer Verlag.
- 4 J. Canny. A computational approach to edge detection. *IEEE Trans. PAMI*, 8(6):679–698, 1986.
- 5 Vicent Caselles, Ron Kimmel, and Guillermo Sapiro. Geodesic active contours. *International Journal of Computer Vision*, 22(1):61–79, 1997.
- 6 O. de Leest, P.M. Rozing, L.A Rozendaal, and F.C.T. van der Helm. The influence of gleno-humeral prosthesis geometry and placement on shoulder muscle forces. *Clinical Orthopedics*, 330:222–233, 1996.
- 7 J. Goffin, K. Van Brussel, K. Martens, J. Vander Sloten, R. Van Audekercke, and M.H. Smet. Three-dimensional computed tomography-based, personalized drill guide for posterior cervical stabilization at c1–c2. *Spine*, 26(12):1343–1347, 2001.
- 8 Xiao Han, Chenyang Xu, and Jerry L. Prince. A topology preserving level set method for geometric deformable models. *IEEE Trans. PAMI*, 25(6):755–768, 2003.
- 9 F. Vega Higuera, N. Sauber, B. Tomandl, C. Nimsky, G. Greiner, and P. Hastreiter. Enhanced 3D-visualization of intracranial aneurysms involving the skull base. In R.E. Ellis and T.M. Peters, editors, *MICCAI 2003*, volume LNCS 2879, pages 256–263. Springer-Verlag Heidelberg, 2003.
- 10 B. Jaramaz, C. Nikou, D. Simon, and A.M. Di Gioia. Range of motion after total hip arthroplasty: Experimental verification of the analytical simulator. Technical Report CMU-RI-TR-97-09, Robotics Institute, Carnegie Mellon University, Pittsburgh, PA, February 1997.
- 11 Yan Kang, Klaus Engelke, and Willi A. Kalender. A new accurate and precise 3-d segmentation method for skeletal structures in volumetric ct data. *IEEE Trans. on Med. Imaging*, 22(5):586–598, 2003.
- 12 Gordon Kindlmann and James W. Durkin. Semi-Automatic Generation of Transfer Functions for Direct Volume Rendering. In *IEEE Symposium on Volume Visualization*, pages 79–86, 1998.
- 13 Peter R. Krekel, Charl P. Botha, Edward R. Valstar, Paul W. de Bruin, Piet M. Rozing, and Frits H. Post. Interactive simulation and comparative visualisation of the bone-determined range of motion of the human shoulder. In *Proceedings of Simulation and Visualization*, March 2006.
- 14 R. Lattanzi, M. Petrone, P. Quadrani, C. Zannoni, and M. Viceconti. Applications of 3d medical imaging in orthopaedic surgery: Introducing the hip-op system. *Proc. First International Symposium on 3D Data Processing Visualization and Transmission*, pages 808–811, June 2002.

- 15 H. Malchau, P. Herberts, P. Söderman, and A. Odén. Prognosis of total hip replacement. Update and validation of results from swedish national hip arthroplasty registry 1979–1998. In *Scientific exhibition presented at the 67th AAOS meeting*, 2000.
- 16 C.G.M. Meskers, F.C.T. van der Helm, L.A. Rozendaal, and P.M. Rozing. *In vivo* estimation of the glenohumeral joint rotation center from scapular bony landmarks by linear regression. *Journal of Biomechanics*, 31:93–96, 1998.
- 17 J.A. Richolt, M. Teschner, P. Everett, B. Girod, M.B. Millis, and R. Kikinis. Planning and evaluation of reorienting osteotomies of the proximal femur in cases of scfe using virtual three-dimensional models. In *MICCAI '98*, pages 1–8, London, UK, 1998. Springer-Verlag.
- 18 Iwo Serlie, Roel Truyen, Jasper Florie, Frits Post, Lucas van Vliet, and Frans Vos. Computed cleansing for virtual colonoscopy using a three-material transition model. In R.E. Ellis and T.M. Peters, editors, *MICCAI 2003*, volume LNCS 2879, pages 175–183. Springer-Verlag Heidelberg, 2003.
- 19 J.A. Sethian. *Level Set Methods and Fast Marching Methods*. Cambridge University Press, 2nd edition, 1999.
- 20 D.A. Simon, B. Jaramaz, M. Blackwell, F. Morgan, A.M. DiGioia, E. Kischell, B. Colgan, and T. Kanade. Development and validation of a navigational guidance system for acetabular implant placement. *Proc. of the First Joint CVRMed / MRCAS Conference*, pages 583–592, 1997.
- 21 Pierre Terdiman. Memory-optimized bounding-volume hierarchies. 2001. <http://www.codercorner.com/Opcode.htm>.
- 22 M.E Torchia, R.H. Cofield, and C.R. Settergren. Total shoulder arthroplasty with the neer prosthesis: long-term results. *Journal of Shoulder and Elbow Surgery*, 6(6):495–505, 1997.
- 23 E.R. Valstar, K van Brussel, B.L. Kaptein, B.C. Stoel, and P.M. Rozing. CT-based personalized templates for accurate glenoid prosthesis placement in total shoulder arthroplasty. In *Proc. CAOS*, 2003.
- 24 Marjolein van der Glas, Frans M. Vos, Charl P. Botha, and Albert M. Vossepoel. Determination of Position and Radius of Ball Joints. In Milan Sonka, editor, *Proceedings of the SPIE International Symposium on Medical Imaging*, volume 4684 - Image Processing, 2002.
- 25 Frans C.T. van der Helm. A finite element musculo-skeletal model of the shoulder mechanism. *Journal of Biomechanics*, 27(5):551–569, 1994.
- 26 Reza A. Zoroofi, Yoshinobu Sato, Toshihiko Sasama, Takashi Nishii, Nobuhiko Sugano, Kazuo Yonenobu, Hideki Yoshikawa, Takahiro Ochi, and Shinichi Tamura. Automated segmentation of acetabulum and femoral head from 3-d ct images. *IEEE Transactions on Information Technology in Biomedicine*, 7(4):329–343, 2003.